Available online at www.sciencedirect.com

ScienceDirect

Mendeleev Commun., 2023, **33**, 37–40

Mendeleev Communications

Halogen-substituted salicylhydroximate copper(II) metallacrowns: from synthesis and structures to novel applications

Marina A. Katkova,*[a] Galina S. Zabrodina,[a] Roman V. Rumyantcev,[a] Grigory Yu. Zhigulin,[a] Maria S. Muravyeva,[a,b] Margarita P. Shurygina,[a,c] Sergey A. Chesnokov[a] and Sergey Yu. Ketkov[a]

[a] *G. A. Razuvaev Institute of Organometallic Chemistry, Russian Academy of Sciences, 603137 Nizhny Novgorod, Russian Federation. E-mail: marina@iomc.ras.ru*
[b] *Privolzhsky Research Medical University, 603005 Nizhny Novgorod, Russian Federation*
[c] *A. M. Butlerov Institute of Chemistry, Kazan Federal University, 420008 Kazan, Russian Federation*

DOI: 10.1016/j.mencom.2023.01.011

New halogen-substituted salicylhydroximate copper(II) metallacrowns were synthesized from $Cu(OAc)_2$ and the corresponding salicylhydroxamic acids. Their molecular structure was determined by single crystal X-ray diffraction. The compounds obtained represent the first members of the metallacrown family that can be used as components of active initiators for the photopolymerization of oligocarbonate dimethacrylate by visible light.

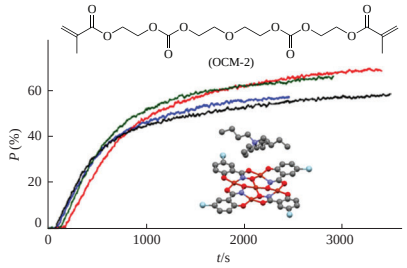

Keywords: copper(II) metallacrowns, organohalogen compounds, salicylhydroxamic acids, X-ray structure, DFT calculations, photopolymerization of dimethacrylate.

To date, metallacrowns (MCs) present an exceptional class of polynuclear metallamacrocyclic complexes that form repeating [M–N–O] subunits with a large variety of fascinating structures of different sizes and topologies.[1–7] Since the first description of these complexes in 1989, salicylhydroxamic acid (H_3shi) has been one of the oldest ligands in such systems.[8] Note that organic ligands based on hydroxamic and 2-hydroxybenzoic acids and their derivatives have received considerable attention due to their synthetic and biological importance.[9–14] Hydroxamic acids of general formula RC(=O)N(R′)OH have a high binding affinity to a range of various metal ions, so studies of their MC complexes still attract great attention.[15] Salicylhydroxamic acid **A** (Figure 1) can act as a bifunctional ligand that provides the nitrogen and oxygen donors to the MC ring metals. The triply deprotonated form shi^{3-} **B** illustrates the four potential metal binding sites. The latter is a chelating-bridging ligand in MC structure, where the first metal can bind in a five-membered chelate ring formed through the hydroximate group, while the second metal can bind to the six-membered substituted iminophenolate ring thus giving structure **C**.[16]

Although copper(II) salicylhydroximate MCs have been reported previously,[17–19] to the best of our knowledge, there have been no investigations on halogen-substituted salicylhydroximate copper(II) MCs. Our interest is focused in the synthesis and characterization of these new halogen-substituted salicylhydroximate copper(II) MCs and their potential applications for acrylate photopolymerization under visible light.

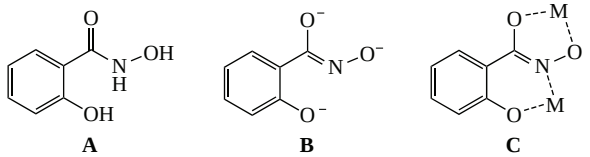

Figure 1 Schematic representations of the species for the metal–salicylhydroxamic acid systems H_3shi (**A**), shi^{3-} (**B**) and [M_2shi] (**C**).

Following the previously described synthetic procedure[19] for copper(II) salicylhydroximate MCs, we employed the most frequently used two-step methodology with some modification (Scheme 1). In the first step, halogen-substituted salicylhydroxamic acid and $Cu(OAc)_2$ were mixed in DMF/MeOH solvents and, in the second step, Bu_4NOH was added to this solution.

The synthesized complexes $(Bu_4N)_2$Cu[12-$MC_{CuN(shi)}$-4] **1**, $(Bu_4N)_2$Cu[12-$MC_{CuN(Clshi)}$-4] **2**, $(Bu_4N)_2$Cu[12-$MC_{CuN(Brshi)}$-4]

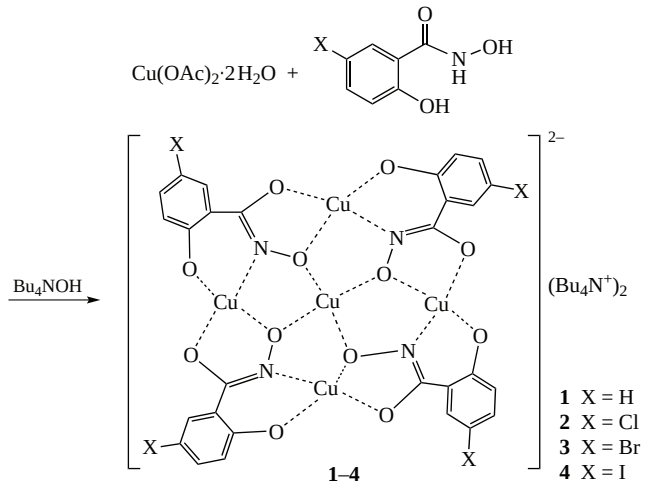

Scheme 1

3, and $(Bu_4N)_2Cu[12\text{-}MC_{CuN(Ishi)}\text{-}4]$ **4** are air-stable, soluble in DMF, DMSO and slightly soluble in methanol (for details, see Online Supplementary Materials). Their UV-VIS spectra are characterized by a wide range of absorption from 300 to *ca.* 650 nm (Figure S1). The stability of complexes **1**–**4** in DMSO solutions at room temperature was confirmed by ^{1}H NMR since such spectra in DMSO-d_6 show well-resolved peaks in the 1–21 ppm region (Figures S2–S4) that do not change with time.

The molecular structures of complexes **1**–**3** were determined by single-crystal X-ray diffraction studies.† The asymmetric unit cell of crystal **1** contains a half of an anionic metallamacrocycle [Figure 2(*a*)] and two halves of tetrabutylammonium cations (Figure 3).

Due to the fact that the central copper atom Cu(1) in MC **1** lies on the symmetry element, it adopts an ideal square planar geometry. Complexes **2** and **3** are isostructural compounds (Table S1). Unlike crystal **1**, the asymmetric unit cells of crystals

† *Crystal data for* **1**. $C_{60}H_{88}Cu_5N_6O_{12}$, M = 1403.06, monoclinic, space group $P2/n$, 100(2) K, a = 18.6359(9), b = 8.1055(4) and c = 19.8079(10) Å, Z = 2, V = 2990.5(3) Å^3, d_{calc} = 1.558 g cm^{-3}, F_{000} = 1462. A green stick-shaped single crystal with dimensions of 0.70 × 0.08 × 0.04 mm was selected, and the intensities of 45566 reflections were measured (ω-scans technique, λ[MoK_α] = 0.71073 Å, μ = 1.816 mm^{-1}, $2\theta_{max}$ = 61.168°). After merging of equivalents and absorption corrections, 9190 independent reflections (R_{int} = 0.0435) were used for the structure solution and refinement. Final R factors: R_1 = 0.0354 [7560 reflections with $I > 2\sigma(I)$], wR_2 = 0.0887 (all reflections), GOF = 1.057.

Crystal data for **2**. $C_{60}H_{88}Cl_4Cu_5N_6O_{14}$, M = 1576.86, monoclinic, space group $P2_1/n$, 100(2) K, a = 18.6623(7), b = 18.3520(7) and c = 18.8978(7) Å, Z = 4, V = 6472.3(4) Å^3, d_{calc} = 1.618 g cm^{-3}, F_{000} = 3260. A black prism-shaped single crystal (0.36 × 0.33 × 0.24 mm) was selected, and the intensities of 65947 reflections were measured (ω-scans technique, λ[MoK_α] = 0.71073 Å, μ = 1.850 mm^{-1}, $2\theta_{max}$ = 57.398°). After merging of equivalents and absorption corrections, 16716 independent reflections (R_{int} = 0.0562) were used for the structure solution and refinement. Final R factors: R_1 = 0.0508 [11636 reflections with $I > 2\sigma(I)$], wR_2 = 0.1395 (all reflections), GOF = 1.027.

Crystal data for **3**. $C_{60}H_{88}Br_4Cu_5N_6O_{14}$, M = 1754.70, monoclinic, space group $P2_1/n$, 100(2) K, a = 18.8048(7), b = 18.5677(7) and c = 18.8166(7) Å, Z = 4, V = 6569.0(4) Å^3, d_{calc} = 1.774 g cm^{-3}, F_{000} = 3548. A black prism-shaped single crystal (0.40 × 0.29 × 0.20 mm) was selected, and the intensities of 146346 reflections were measured (ω-scans technique, λ[MoK_α] = 0.71073 Å, μ = 4.093 mm^{-1}, $2\theta_{max}$ = 60.068°). After merging of equivalents and absorption corrections, 19195 independent reflections (R_{int} = 0.0389) were used for the structure solution and refinement. Final R factors: R_1 = 0.0314 [15851 reflections with $I > 2\sigma(I)$], wR_2 = 0.0721 (all reflections), GOF = 1.047.

The X-ray diffraction data were collected on a Bruker D8 Quest diffractometer using the APEX3 software package. The intensity data were integrated by SAINT[20] program. SADABS program[21] was used to perform absorption corrections. All structures were solved by dual method[22] and refined on F^2_{hkl} using SHELXTL package.[23] All non-hydrogen atoms were refined anisotropically. The hydrogen atoms, except for the hydrogen atoms in water molecules in **2** and **3**, were placed in calculated positions and were refined in the riding model [U_{iso}(H) = 1.5 U_{eq}(C) for CH_3-groups and U_{iso}(H) = 1.2 U_{eq}(C) for other groups]. In turn, the hydrogen atoms in all water molecules in crystals **2** and **3** were found from Fourier syntheses of electron density. The DFIX instruction was used to refine the hydrogen atoms of water. Thermal ellipsoids have been fixed to 1.2 U_{eq}(O). The metallamacrocycle in **1** is disordered over two positions with site occupancies of 0.85 : 0.15. The disordered molecule in crystal **1** was modeled and refined with restraints of thermal parameters (EADP and ISOR). There are two uncoordinated water molecules per metallamacrocycle in crystals **2** and **3**. All figures were generated with the program Mercury.[24]

CCDC 2166112 (**1**), 2169294 (**2**) and 2169295 (**3**) contain the supplementary crystallographic data. These data can be obtained free of charge from The Cambridge Crystallographic Data Centre *via* http://www.ccdc.cam.ac.uk.

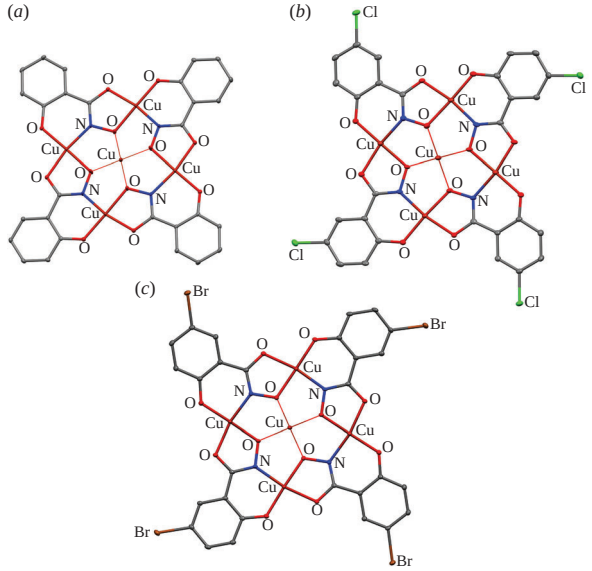

Figure 2 The molecular structures of the anionic part for (*a*) complex **1**, (*b*) complex **2** and (*c*) complex **3**. The thermal ellipsoids are drawn at the 30% probability level. All hydrogen atoms are omitted.

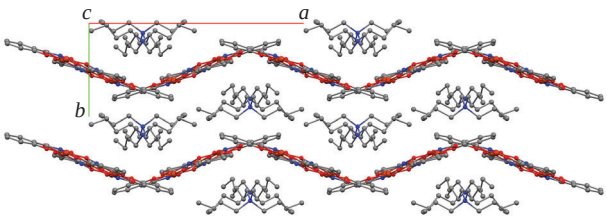

Figure 3 Fragment of crystal packing along the crystallographic *c* axis of complex **1**. The hydrogen atoms are omitted for clarity.

2 and **3** contain an anionic metallamacrocycle and two tetrabutylammonium cations [see Figures 2(*b*),(*c*), 4, S5].

The introduction of halogen atoms into the metallamacrocycle in complexes **2** and **3** slightly affects the main geometric characteristics (Tables 1 and S2). The Cu(1)–O(oxime) distances vary within range of 1.858(8)–1.910(2) Å and are in good agreement with related copper complexes.[17,18,25] In all three complexes **1**–**3**, the metallamacrocycle anion is almost flat. Despite the fact that the maximum deviation of atoms from the plane is 0.377, 0.638 and 0.668 Å in complexes **1**, **2** and **3**, the average deviation of non-hydrogen atoms is 0.142, 0.156 and 0.163 Å, respectively. The central copper atom Cu(1) in complex **1** lies in the plane of the MC. In turn, in complexes **2** and **3** there is a deviation of the central copper atom from the plane of the MC by 0.142 and 0.149 Å. The nitrogen atoms in tetrabutylammonium cations adopt an almost ideal tetrahedral

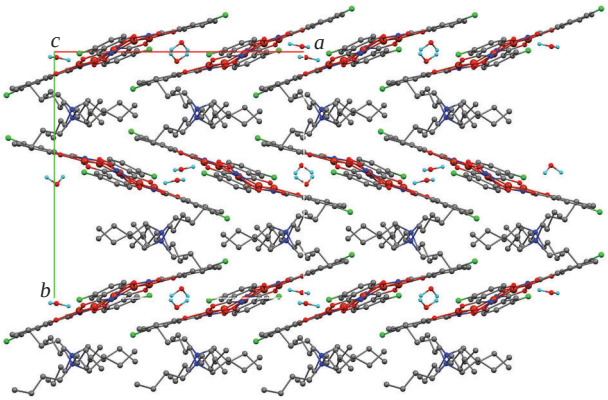

Figure 4 Fragment of crystal packing along the crystallographic *c* axis of complex **2**. The hydrogen atoms are omitted for clarity.

Table 1 Selected bond lengths (Å) in complexes **1**, **2** and **3**.

Distance/Å	**1**	**2**	**3**
Cu(1)–O(oxime)	1.858(8)–1.889(9)	1.865(2)–1.905(2)	1.861(2)–1.910(2)
Cu–O(oxime)	1.894(2)–1.897(2)	1.878(2)–1.917(3)	1.888(2)–1.919(2)
Cu–O(carbonyl)	1.947(2)–1.956(2)	1.944(2)–1.958(2)	1.944(2)–1.959(2)
Cu–O(phenolate)	1.864(2)–1.871(2)	1.870(2)–1.887(3)	1.873(2)–1.886(2)
Cu–N(imine)	1.930(2)–1.934(2)	1.917(3)–1.930(3)	1.915(2)–1.933(2)
C–Hal	–	1.745(4)–1.752(4)	1.904(2)–1.908(2)

geometry. All C–C and C–N bonds in cations vary in normal range.[26]

In crystal **1**, MC molecules are arranged in such a way that intermolecular H···O interactions (2.467, 2.577 Å) are realized with four neighboring metallamacrocycles[27] (Figure S6). As a result, an endless 2D network of negatively charged MCs surrounded by cations is formed (see Figure 3). The planes of neighboring metallamacrocycles form a dihedral angle of 39.3°. Unlike crystal **1**, MCs of **2** and **3** form infinite molecular chains (Figure S7). The distances between the center of the phenyl ring of one MC molecule and copper atom of the neighboring MC are 3.503 and 3.508 Å in **2**, 3.525 and 3.555 Å in **3**. Additionally, neighboring MC molecules in the chain are connected to each other *via* intermolecular O···H interactions (1.956 and 2.209 Å in **2**, 1.949 and 2.125 Å in **3**) with solvate water molecules. Molecular chains of metallamacrocycles in the crystal form layers separated by tetrabutylammonium cations (see Figure 4). The planes of MC molecules in neighboring layers form a dihedral angle of 40.44 and 40.54° in crystals **2** and **3**.

Influence of the halogen substituents on the electronic structures of the metallamacrocycles was investigated with the Gaussian 09 software.[28] The corresponding geometries of the H-, Cl-, Br-, and I-substituted dianionic metallamacrocycles were fully optimized in the sextet spin state at the B3LYP/DGDZVP level of DFT. The combination of the B3LYP functional[29–31] and DGDZVP basis set[32,33] has been shown to be a good choice for description of the paramagnetic hydroximate metallamacrocycles.[34–37] Structural parameters of the optimized species are close to the values obtained from the X-ray crystallographic experiment. In particular, the Cu–N(imine) distances calculated for all the four metallamacrocycles lie in the range of 1.944–1.954 Å, being slightly shorter than the Cu–O(carbonyl) bonds (1.990–1.994 Å). The computed C–Hal distances are identical within each structure: 1.780, 1.939, and 2.144 Å for the Cl-, Br-, and I-derivative, respectively. The electron-accepting influence of the halogens is confirmed by the molecular electrostatic potential (MEP) distribution revealing a shift of electron density from the metallamacrocycle to the peripheral halogen substituents (Figure 5). In the halogenated derivatives, the negative red regions around the oxygen atoms decrease in size, the aromatic rings become more positive (green coloring), and the blue sites corresponding to the copper cations are seen more clearly. Moreover, the most positive blue regions of MEP cover not only the copper ions but also hydrogen atoms and σ-holes[38] of the halogen atoms. Thus, even in the metallamacrocycles bearing the 2– charge the electron-accepting halogen atoms do not gain enough electron density to quench their σ-holes.

MO analysis of the metallamacrocycles detects β-HOMO to be characterized by the maximum energy among the occupied α- and β-orbitals. On substituent variation the energy gap between β-HOMO and β-LUMO remains practically unchanged being in the range of 1.91–1.93 eV, with both β-HOMO and β-LUMO containing contributions of copper *d*-orbitals (Figures 6 and S8).

Calculated β-HOMO–β-LUMO gaps agree well with the position of the *d*–*d* absorption band at 620 nm (2.00 eV) in the

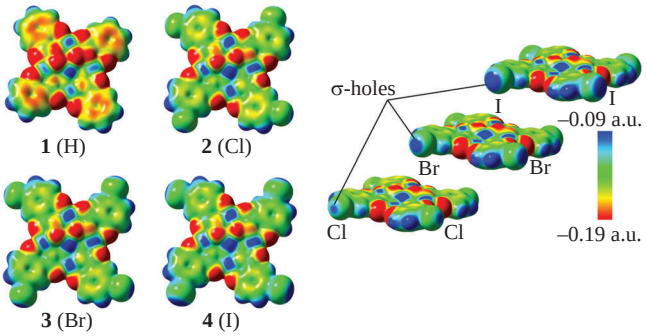

Figure 5 MEP distribution mapped on the electron density isosurface (0.005 atomic units) for the DFT optimized structures of the dianionic metallamacrocycles **1**–**4**.

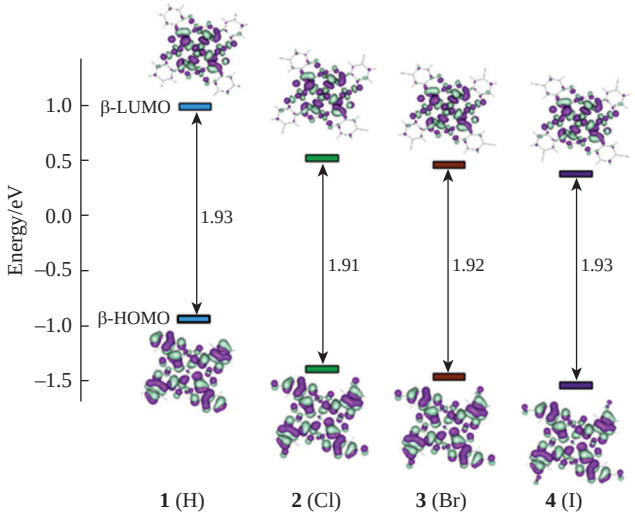

Figure 6 Isosurfaces (at 0.018) and energies (in eV) of the frontier molecular β-orbitals for the DFT optimized structures of the dianionic metallamacrocycles **1**–**4**.

UV-VIS spectra of the H-, Cl-, Br-, and I-derivatives. On the other hand, introduction of the halogen substituents decreases the energies of β-HOMO and β-LUMO indicating the electron-accepting effect of the halogens. In particular, on going from the H- to Cl-substituted metallamacrocycle β-HOMO and β-LUMO energies decrease by 0.45 and 0.47 eV, respectively.

Since copper complexes gain great interest as visible light photosensitizers, we decided to demonstrate the potential use of our complexes **1**–**4** in photopolymerization of oligocarbonate dimethacrylate (OCM-2). The photopolymerization process was carried out under irradiation of low-energy light sources LEDs@385,405 nm exposure (25 mW cm^{-2}), T = 298 K, in air.[39] The kinetic results of photopolymerization of OCM-2 in the presence of **1**–**4** alone (Figure S9) indicate their insignificant photoinitiating activity. The maximum rate of photopolymerization by **3** is $W_{max} = 1.4 \times 10^{-5}$ s^{-1}, and the maximum conversion P is near 10%. In contrast, the addition of triethylamine (TEA) to photopolymerized composition (PPC) leads to a significant increase in the final conversions and rates. The W_{max} value increases by an order to 2.7×10^{-4} s^{-1} with injection of 1 vol% TEA. Upon the addition of 10 vol% TEA into the PPC, the maximum photopolymerization rate increases by a factor of three to $W_{max} = 8.1 \times 10^{-4}$ s^{-1}. The polymerization profiles (acrylate function conversion *vs.* irradiation time) for OCM-2 in the presence of MCs **1**–**4** with TEA are shown in Figure 7.

From the kinetics data presented in Figure 7 and summarized in Table 2, it can be concluded that the nature of the substituent in the MC has a significant influence on the duration of the induction period. For example, the induction period (t_{ind}) for **2** (Cl) is twice

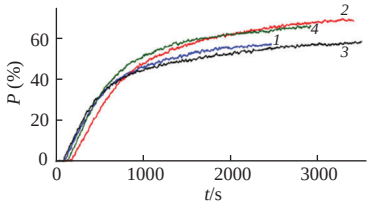

Figure 7 Polymerization profiles (acrylate function conversion *vs.* irradiation time) for OCM-2 in the presence of MC/TEA system: (*1*) **1**/TEA, (*2*) **2**/TEA, (*3*) **3**/TEA, (*4*) **4**/TEA. [MC] = 1.3×10^{-4} M, [TEA] = 10 vol%.

Table 2 Kinetic parameters of OCM-2 photopolymerization in the presence of MC/TEA initiating systems ([MC] = 1.3×10^{-4} M, [TEA] = 10 vol%).

MC/TEA	t_{ind}/s	$W_{max} \times 10^4$/s^{-1}	*P* (%)
1	110	7.1	64
2	190	7.0	69
3	95	8.1	59
4	150	8.4	67

longer than that for **3** (Br). At the same time, the conversion of photopolymerization in the presence of **2** is 10% higher than that for **3**. The rate of photopolymerization (W_{max}) depends slightly on the MC nature. Thus, a combination of **3** with TEA can be considered as the optimal photoinitiating system.

In summary, new halogen-substituted salicylhydroximate copper(II) metallacrowns have been synthesized and structurally characterized. They represent the first members of the metallacrown family that can be employed as components of photoinitiators for the polymerization of oligocarbonate dimethacrylate OCM-2 with the visible light. The current results can be used as a basis for further development of environmentally friendly procedure of acrylate polymerization.

The synthetic, structural and theoretical parts of this work were supported by the Russian Science Foundation (grant no. 18-13-00356). The polymerization studies were carried out in accordance with the Strategic Academic Leadership Program ‘Priority 2030’ of the Kazan Federal University of the Government of the Russian Federation. The experimental investigation was carried out using the equipment of the center for collective use ‘Analytical Center of the IOMC RAS’ with the financial support of the grant ‘Ensuring the development of the material and technical infrastructure of the centers for collective use of scientific equipment’ (unique identifier RF-2296.61321X0017, agreement no. 075-15-2021-670).

Online Supplementary Materials

Supplementary data associated with this article can be found in the online version at doi: 10.1016/j.mencom.2023.01.011.

References

1 M. S. Lah and V. L. Pecoraro, *Comments Inorg. Chem.*, 1990, **11**, 59.
2 J. J. Bodwin, A. D. Cutland, R. G. Malkani and V. L. Pecoraro, *Coord. Chem. Rev.*, 2001, **216**–**217**, 489.
3 G. Mezei, C. M. Zaleski and V. L. Pecoraro, *Chem. Rev.*, 2007, **107**, 4933.
4 M. Tegoni and M. Remelli, *Coord. Chem. Rev.*, 2012, **256**, 289.
5 M. Ostrowska, I. O. Fritsky, E. Gumienna-Kontecka and A. V. Pavlishchuk, *Coord. Chem. Rev.*, 2016, **327**–**328**, 304.
6 Y. Pavlyukh, E. Rentschler, H. J. Elmers, W. Hübner and G. Lefkidis, *Phys. Rev.*, 2018, **B97**, 214408.
7 M. A. Katkova, *Russ. J. Coord. Chem.*, 2018, **44**, 284 (*Koord. Khim.*, 2018, **44**, 135).
8 M. S. Lah and V. L. Pecoraro, *J. Am. Chem. Soc.*, 1989, **111**, 7258.
9 R. Codd, *Coord. Chem. Rev.*, 2008, **252**, 1387.
10 S. P. Gupta, *Chem. Rev.*, 2015, **115**, 6427.
11 L. M. Nguyen, H. H. Truong, V. N. Khrustalev, S. T. Truong, D. T. Nguyen, V. T. T. Tran, S. T. Mai, V. T. Tran and A. T. Le, *Mendeleev Commun.*, 2020, **30**, 753.
12 A. D. Zubenko, B. V. Egorova, L. S. Zamurueva, S. N. Kalmykov and O. A. Fedorova, *Mendeleev Commun.*, 2021, **31**, 194.
13 P. A. Panchenko, Yu. V. Fedorov, A. S. Polyakova and O. A. Fedorova, *Mendeleev Commun.*, 2021, **31**, 517.
14 P. A. Panchenko, P. A. Ignatov, M. A. Zakharko, Yu. V. Fedorov and O. A. Fedorova, *Mendeleev Commun.*, 2020, **30**, 55.
15 P. Happ, C. Plenk and E. Rentschler, *Coord. Chem. Rev.*, 2015, **289**–**290**, 238.
16 C. Dendrinou-Samara, G. Psomas, L. Iordanidis, V. Tangoulis and D. P. Kessissoglou, *Chem. – Eur. J.*, 2001, **7**, 5041.
17 C. Plenk, J. Krause, M. Beck and E. Rentschler, *Chem. Commun.*, 2015, **51**, 6524.
18 P. Happ and E. Rentschler, *Dalton Trans.*, 2014, **43**, 15308.
19 J. Herring, M. Zeller and C. M. Zaleski, *Acta Crystallogr.*, 2011, **E67**, m419.
20 *SAINT, Data Reduction and Correction Program, version 8.27B*, Bruker AXS, Madison, WI, 2014.
21 L. Krause, R. H. Irmer, G. M. Sheldrick and D. Stalke, *J. Appl. Crystallogr.*, 2015, **48**, 3.
22 G. M. Sheldrick, *Acta Crystallogr., Sect. A: Found. Adv.*, 2015, **71**, 3
23 G. M. Sheldrick, *Acta Crystallogr., Sect. C: Struct. Chem.*, 2015, **71**, 3.
24 C. F. Macrae, I. Sovago, S. J. Cottrell, P. T. A. Galek, P. McCabe, E. Pidcock, M. Platings, G. P. Shields, J. S. Stevens, M. Towler and P. A. Wood, *J. Appl. Crystallogr.*, 2020, **53**, 226.
25 B. R. Gibney, D. P. Kessissoglou, J. W. Kampf and V. L. Pecoraro, *Inorg. Chem.*, 1994, **33**, 4840.
26 J. F. do Prado, A. K. Valdo, F. T. Martins, R. C. de Santana and D. Cangussu, *J. Mol. Struct.*, 2019, **1203**, 127468.
27 D. Ž. Veljković, *J. Mol. Graphics Modell.*, 2018, **80**, 121.
28 M. J. Frisch, G. W. Trucks, H. B. Schlegel, G. E. Scuseria, M. A. Robb, J. R. Cheeseman, G. Scalmani, V. Barone, B. Mennucci, G. A. Petersson, H. Nakatsuji, M. Caricato, X. Li, H. P. Hratchian, A. F. Izmaylov, J. Bloino, G. Zheng, J. L. Sonnenberg, M. Hada, M. Ehara, K. Toyota, R. Fukuda, J. Hasegawa, M. Ishida, T. Nakajima, Y. Honda, O. Kitao, H. Nakai, T. Vreven, J. A. Montgomery, Jr., J. E. Peralta, F. Ogliaro, M. Bearpark, J. J. Heyd, E. Brothers, K. N. Kudin, V. N. Staroverov, T. Keith, R. Kobayashi, J. Normand, K. Raghavachari, A. Rendell, J. C. Burant, S. S. Iyengar, J. Tomasi, M. Cossi, N. Rega, J. M. Millam, M. Klene, J. E. Knox, J. B. Cross, V. Bakken, C. Adamo, J. Jaramillo, R. Gomperts, R. E. Stratmann, O. Yazyev, A. J. Austin, R. Cammi, C. Pomelli, J. W. Ochterski, R. L. Martin, K. Morokuma, V. G. Zakrzewski, G. A. Voth, P. Salvador, J. J. Dannenberg, S. Dapprich, A. D. Daniels, O. Farkas, J. B. Foresman, J. V. Ortiz, J. Cioslowski and D. J. Fox, *Gaussian 09, Revision E.01*, Gaussian, Wallingford, CT, 2013.
29 D. Becke, *J. Chem. Phys.*, 1993, **98**, 5648.
30 C. Lee, W. Yang and R. G. Parr, *Phys. Rev. B*: *Condens. Matter Mater. Phys.*, 1988, **37**, 785.
31 P. J. Stephens, F. J. Devlin, C. F. Chabalowski and M. J. Frisch, *J. Phys. Chem.*, 1994, **98**, 11623.
32 N. Godbout, D. R. Salahub, J. Andzelm and E. Wimmer, *Can. J. Chem.*, 1992, **70**, 560.
33 C. Sosa, J. Andzelm, B. C. Elkin, E. Wimmer, K. D. Dobbs and D. A. Dixon, *J. Phys. Chem.*, 1992, **96**, 6630.
34 M. A. Katkova, G. S. Zabrodina, G. Yu. Zhigulin, R. V. Rumyantsev and S. Yu. Ketkov, *Russ. J. Coord. Chem.*, 2019, **45**, 721 (*Koord. Khim.*, 2019, **45**, 627).
35 G. Yu. Zhigulin, G. S. Zabrodina, M. A. Katkova and S. Yu. Ketkov, *Russ. J. Coord. Chem.*, 2019, **45**, 356 (*Koord. Khim.*, 2019, **45**, 306).
36 G. Yu. Zhigulin, G. S. Zabrodina, M. A. Katkova and S. Yu. Ketkov, *Russ. Chem. Bull.*, 2018, **67**, 1173.
37 M. A. Katkova, G. S. Zabrodina, E. V. Baranov, M. S. Muravyeva, E. A. Kluev, A. S. Shavyrin, G. Yu. Zhigulin and S. Yu. Ketkov, *Appl. Organomet. Chem.*, 2018, **32**, e4389.
38 T. Clark, M. Hennemann, J. S. Murray and P. Politzer, *J. Mol. Model.*, 2007, **13**, 291.
39 M. Yu. Zakharina, Yu. V. Chechet, M. P. Shurygina and S. A. Chesnokov, *Polym. Sci., Ser. B*, 2018, **60**, 708.

Received: 7th June 2022; Com. 22/6927